Pore Structural Effects in Catalytic Gasification of Coal Chars

The effect of pore structure on the gasification of two chars impregnated with potassium carbonate catalyst is investigated. Well-characterized char samples were reacted with carbon dioxide, water vapor, and oxygen. The effects of catalyst on the magnitude of the gasification rate as well as on the entire rate vs. conversion pattern are reported. Reactivity and structural data are analyzed to obtain a meaningful comparison of the gasification behavior for all char-gas pairs. Initial intraparticle catalyst dispersion was strongly influenced by the pore structure of the chars. During gasification with carbon dioxide and water, the catalyst appeared to redistribute itself in accordance to the accepted reaction mechanism, leading to superior catalytic activity. The reported measurements indicate that both the pore structure of the chars and the chemistry of a particular reaction are key factors in determining the overall catalytic performance.

Girish Ballal, N. R. Amundson
Department of Chemical Engineering
University of Houston
Houston, TX 77004

Kyriacos Zygourakis
Department of Chemical Engineering
Rice University
Houston, TX 77251

Introduction

The catalytic effect of inorganic compounds on the gasification of carbonaceous materials has been studied by several investigators due to the potential of these reactions in coal utilization processes. Among the various metallic compounds, alkali metal salts have shown considerable promise for use in commercial gasifiers due to their relative abundance and superior catalytic properties. Potassium carbonate is thought to be especially suitable as it represents the necessary balance between low cost and high catalytic activity. The present study is aimed at evaluating the catalytic properties of potassium carbonate during various heterogenous gasification reactions of two coal-derived chars.

Despite many previous investigations, the catalytic gasification of coal-derived chars remains poorly understood due to the myriad of factors affecting these processes. The complex pore structure of chars is one of these factors. Direct and indirect measurements on coal chars reveal pores ranging from large vesicles many microns in diameter to fine micropores with dimensions approaching the molecular sizes of commonly used adsorbents. The rank and origin of parent coal, as well as the devolatilization conditions, strongly affect the pore structure and thus the reactivity of chars. The chemical properties of chars are also complicated due to the presence of varying amounts of inorganic impurities in the form of ash. All these factors can make a meaningful analysis of reactivity data extremely difficult even without the presence of catalytic additives.

Another important factor affecting the reactivity of a char is the temporal evolution of its pore structure. As the carbon is depleted during reaction, the pores grow and coalesce with their neighbors. Consequently, the internal surface area, the concentration of available active sites, and the reactivity change drastically with carbon conversion. The transient nature of gasification implies that the initial enhancement of reaction rates due to addition of catalysts may not correctly indicate the levels of catalytic activity throughout the entire range of carbon conversion. Therefore, the entire rate vs. conversion patterns for catalyst-impregnated chars must be measured and compared in order to make meaningful comparisons of catalyst performance.

In addition to the factors relating to the physical and chemical structure of chars, the gasification process is greatly influenced by the gaseous environment. During commercial gasification processes, the char particle undergoes heterogeneous reactions with several gaseous species. The various chemical reactions may follow entirely different reaction pathways and may proceed through the formation of different intermediate species. Since both the rate of gasification and the catalytic performance may be greatly affected by the reaction mechanisms, any conclusions regarding the effectiveness of a catalyst during a particular char-gas reaction cannot be generalized to other

Correspondence concerning this paper should be addressed to Kyriacos Zygourakis.

reactions of the same char. Therefore, a systematic study of all these heterogeneous char-gas reactions is essential for proper evaluation of the performance of the catalyst.

Previous Work and Objectives of Current Study

Some of the earlier developments regarding the catalytic gasification of various carbonaceous compounds are extensively reviewed by Wen (1980) and McKee (1981). More recently, Spiro et al. (1983) studied the catalytic reactions of several chars with CO_2 in the presence of four alkali metal carbonates. The catalytic activity of these chars was compared to that of graphite powder at similar reaction temperatures. Substantial differences in the gasification behavior of graphite and coal-derived chars were observed and they were attributed to the complex physicochemical structure of chars. Similar experimental measurements were reported by Huhn et al. (1983) for water gasification of coal chars impregnated with various alkali metal salts.

Only one reaction (either char-CO_2 or char-H_2O) was studied in each of the above investigations and the catalytic performance was compared on the basis of average gasification rates. Such treatment implicitly assumes homogeneous catalyst impregnation leading to uniform increase in the reactivity throughout the entire char particle. However, the catalytic gasification is indeed a heterogeneous process due to the transient nature of char pore structure and to the possibly nonuniform intraparticle dispersion of the catalyst. Both these factors can lead to substantial changes in the magnitude of catalytic effects during gasification for a particular char-gas system.

Su and Perlmutter (1985a, b) examined the effect of char pore structure on the combustion of bituminous chars in the presence of alkali metal carbonates. The macro- and micropore structures were characterized by mercury penetration and by CO_2 adsorption, respectively. The catalyst was reported to reside entirely on the particle exterior, with negligible penetration inside the particle. Their study, however, included only one gaseous reactant (oxygen) and hence the performance of the catalyst could not be evaluated and compared for other heterogeneous char gasification reactions. Most of the presented reactivity data were also confined to chars obtained from a single parent coal.

Results from a comprehensive experimental study of the catalytic gasification of two chars with three gaseous reactants are presented here. Our work aims at elucidating:

a. The magnitude of catalytic effect at various loadings

b. The effect of catalyst on the entire rate vs. conversion curve for three important char-gas reactions carried out on well-characterized char samples

The two chars employed for the reactivity studies were produced from a lignite and a bituminous coal and have widely different pore structures. Detailed pore structural measurements were carried out on both the catalyst-impregnated and the nonimpregnated char samples. The results presented will illustrate how the pore structure affects the intraparticle distribution of catalytic additives and, consequently, the char reactivities during catalytic gasification.

Gasification of the same two chars with CO_2, O_2, and water vapor in the absence of catalytic additives has been studied extensively in our previous investigations (Ballal and Zygourakis 1986, 1987a). The present study extends these measurements to char samples impregnated with potassium carbonate and gasified with CO_2, O_2, and water vapor. By analyzing all the experimental reactivity data, one can obtain meaningful comparisons of the catalytic activity when a particular char is gasified in different gaseous environments. The reactivity measurements were continued until complete conversion in order to investigate the effects of pore structural changes on char reactivity and to evaluate the performance of the catalyst over the entire range of carbon conversion.

Experimental Procedures

Char preparation and structural characterization

Two chars were prepared from a Texas lignite and a Pittsburgh #8 bituminous coal in a batch fluidized-bed reactor using nitrogen as a carrier gas (Ballal, 1985). The bed was heated at about 10°C/min to a final temperature of 900°C (particle size 275 μm). Volatile matter was almost completely removed during this process, as indicated by the proximate analysis of char samples given in Table 1. The lignite char contains considerably larger amounts of inorganic impurities (ash) as compared to the Pittsburgh #8 char.

A battery of analytical techniques was employed to accurately characterize the macro- and micropore structures. Macropores larger than 0.5 μm were analyzed via optical microscopy and digital image processing (Glass and Zygourakis, 1987). Digitized (binary) images of representative particle cross sections from the two char samples are shown in Figure 1. The lignite char exhibits a pervious pore structure with a large number of interconnected macropores. Macropores are larger and fewer for the Pittsburgh #8 char and they are separated from each other by a relatively dense carbon matrix. The macropore structure was also quantitatively characterized by the mercury penetration method using pressures up to 10,000 psi (68.9 MPa) in order to obtain volumes and surface areas of pores larger than 20 nm. Pore size analysis via image processing shows

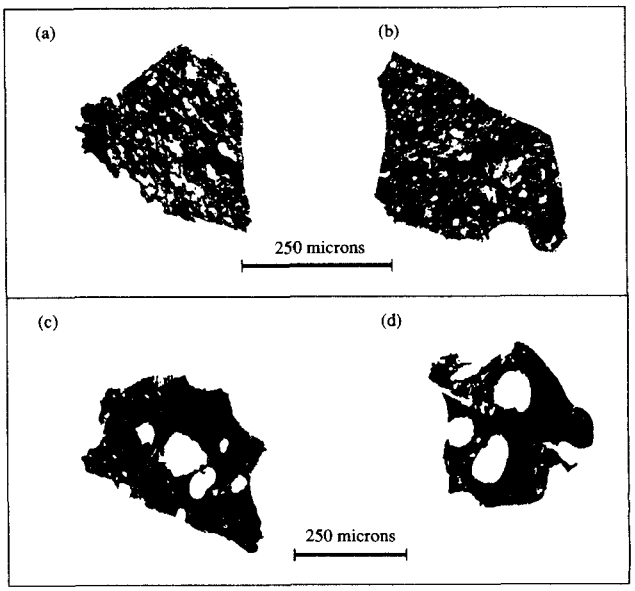

Figure 1. Digitized images of char particle cross sections.
Black denotes the carbon matrix, white areas correspond to macropore sections
(a, b) Lignite char
(c, d) Pittsburgh #8 char

that the Pittsburgh #8 char contains significantly less macropore volume and area as compared to the lignite char (Glass and Zygourakis, 1987)

Several gas adsorption techniques were used to analyze the micropore structure. These measurements using N_2 adsorption at 77 K (BET analysis) and CO_2 adsorption at 298 K (DP analysis) are also reported in Table 1. The micropore capacities of the Pittsburgh #8 char calculated from these two techniques are vastly different. This observation implies that this char contains a large number of fine micropores that are inaccessible to N_2 molecules at 77 K. The detailed description of the micropore structure and its implications on the char reactivity-conversion patterns were presented in detail in an earlier publication (Ballal and Zygourakis, 1987a).

Although these equilibrium adsorption measurements provide important pore structural properties such as pore volumes and surface areas, they do not directly indicate how easily the diffusing gas molecules can penetrate the pore structure. The bidisperse pore structure of chars complicates the study of intraparticle mass transport rates. Paths of low resistance to the diffusing species are provided by the network of large macropores, which act as arteries to distribute adsorbants or reactants throughout the particle. Most of the available surface area, however, lies in the micropores and large resistances to mass transfer are encountered as the gaseous reactants diffuse from the macropore network into the microporous solid. Due to the small size of the micropores, diffusion in them is many times slower than diffusion in the macropore network. The effective mass transport rates are thus determined by several factors related to the details of the micro- and macropore structures.

The diffusional resistances for both chars were estimated in this study from transient gas adsorption experiments conducted at room temperature in a closed system (Ballal, 1985). Under these conditions, diffusion in the large cavities is extremely fast (as compared to diffusion in the micropores) and can be assumed to be instantaneous. Hence, the transient adsorption measurements are essentially controlled by the diffusional resistance of the microporous solid separating the large cavities. The microporous regions (or microparticles) are surrounded by macropores and it can thus be assumed that the gaseous concentration on the outside surface of the microparticles is equal to the bulk concentration of the adsorbant. Transient on-line measurements of the bulk gaseous concentrations provide the flux of the diffusing gaseous species in the microparticles and allow the estimation of a transport parameter D_e/R^2, where D_e represents the effective diffusivity inside the microparticle of radius R. The effective microparticle radius, R, depends strongly on the compactness of the macropore structure and it is larger when the macrocavities are widely separated from each other. Thus, both the micro- and macropore structures affect the parameter D_e/R^2, which can be used to quantify intraparticle mass transfer rates.

Table 1. Proximate Analysis and Pore Structural Properties of Chars

	Lignite	Pittsburgh #8
Proximate Analysis		
Moisture, %	3.43	1.14
Volatile matter, %, mf	3.70	1.90
Ash, %, mf	39.9	18.6
Fixed carbon, %, mf*	56.4	79.5
Helium Density, g/cm^3	1.76	2.10
Mercury Porosimetry		
Surface area, m^2/g	6.33	1.97
Pore volume, cm^3/g	0.105	0.029
N_2 Adsorption (BET)		
Surface area, m^2/g	182.0	4.8
Pore volume, cm^3/g	0.105	3.03×10^{-3}
CO_2 Adsorption (DP)		
Surface area, m^2/g	488.7	334.6
Pore volume, cm^3/g	0.090	0.062
Diffusion Parameter		
D/R^2, 1/s	150×10^{-5}	1.75×10^{-5}

*Calculated by difference

Figure 2 presents the transient measurements for CO_2 adsorption on the two chars at room temperature. The Pittsburgh #8 char clearly exhibits considerably larger resistance to diffusion than the lignite char. This is primarily due to the dissimilar macropore structures of these two chars. Figures 1a and 1b illustrated the extremely pervious macropore structure of the lignite char. On the other hand, the Pittsburgh #8 char exhibits large cavities separated by large dense microporous regions, Figures 1c and 1d. Therefore, the latter char is characterized by large microparticle sizes and is expected to offer considerably larger resistance to transport. Diffusion parameters were estimated from these experimental measurements and are listed in Table 1. Since diffusion in the lignite char was extremely fast, the diffusion parameter reported for this char should only be taken as a rough estimate. Nevertheless, the relative magnitudes of the transport parameters unequivocally point out the widely different overall transport resistances offered by the two chars.

Catalyst impregnation

The chars were impregnated with the catalyst from an aqueous solution of potassium carbonate at room temperature and

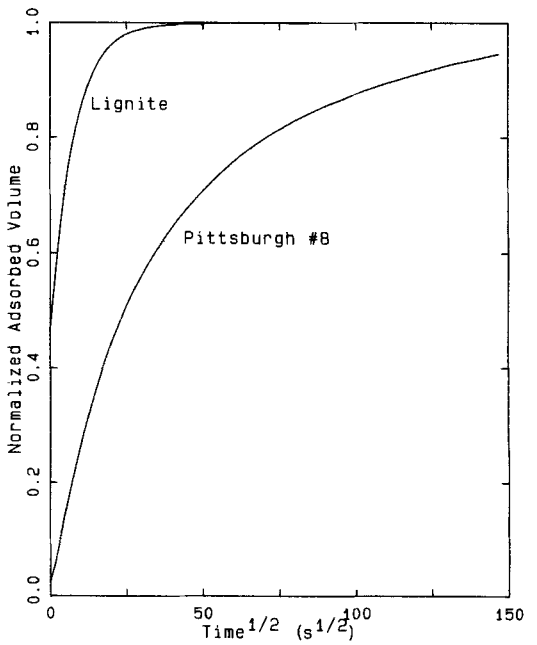

Figure 2. Transient measurements of CO_2 adsorption on lignite and Pittsburgh #8 chars.

were allowed to dry overnight before being placed in a desiccator for further drying and storage. Samples with four catalyst loadings were obtained from each char using different concentrations of the impregnating solution.

CO_2 adsorption experiments were carried out on two samples to examine the effect of catalyst impregnation on the micropore structure. Since CO_2 can penetrate even fine micropores at 25°C, any substantial blockage of these pores due to the catalyst particles should result in a reduction of the micropore capacity measured from the CO_2 adsorption isotherm. Figure 3 shows the linearized adsorption isotherms obtained for catalyst-impregnated and nonimpregnated samples of the lignite and Pittsburgh #8 chars. Since the isotherms obtained for the impregnated and nonimpregnated samples are almost identical, yielding similar accessible micropore volumes, one can conclude that the catalyst did not block the micropores of these samples to any appreciable extent. Su and Perlmutter (1985a) conducted similar experiments on chars impregnated with sodium and potassium carbonates from aqueous solutions and also found that catalyst addition caused insignificant blockage of the micropores.

Reactivity measurements

A thermogravimetric reactor was used for the reactivity measurements. A computer-automated data acquisition and control system was interfaced to the TGA to heat the sample quickly to the final reaction temperature and to facilitate the reactivity measurements. Gas of the desired composition was allowed to flow over the sample (maintained at 120°C) for 2 h in order to remove moisture and to flush the apparatus. The sample was heated at 160°C/min to the desired reaction temperature, and the temperature was maintained constant thereafter. All runs were continued until almost complete conversion and the experimental measurements were transferred to a VAX 11-750 minicomputer for further analysis.

Results and Discussion

Dispersion of catalyst in the char particles

The widely different macropore structures of the two chars resulted in dissimilar diffusional rates and diffusion parameters during the adsorption of CO_2 at room temperature. Similar behavior is also expected for the diffusion of catalyst during impregnation. The catalyst rapidly disperses throughout the macropore network for both chars. The closely interconnected previous macropore structure of the lignite char ensures fairly uniform distribution of the catalyst throughout the particle. The Pittsburgh #8 char, however, contains large dense microporous regions separating the large cavities. Due to the extremely slow diffusional rates in its microporous structure the catalyst can permeate only in a small neighborhood of the surface of large cavities. Consequently, a nonuniform dispersion of the catalyst is expected with catalyst-rich regions forming in the immediate vicinity of the macropores and near the external surface of the particle. The rest of the particle is likely to contain relatively small catalyst concentration.

These arguments were verified by scanning electron microscopy (SEM) studies. Polished cross sections of catalyst-impregnated particles were analyzed to obtain information on the distribution of potassium in the macroscopic scale. As expected, most of the potassium present in Pittsburgh #8 char particles was found to reside on the exterior of the particle as well as near the edges of the large cavities. A more uniform dispersion of the potassium was observed in the lignite char particles.

Char reactivities during noncatalytic gasification

Ballal and Zygourakis (1987a) studied the evolution of reactivities of various well-characterized coal chars during gasification with CO_2 and O_2. These studies were later extended to gasification with water vapor. A wide spectrum of reaction con-

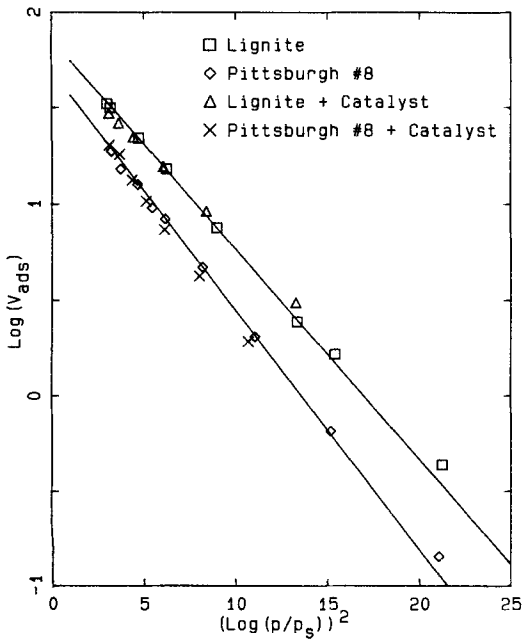

Figure 3. Linearized Dubinin-Polanyi plots for CO_2 adsorption showing effect of catalyst impregnation on micropore structure.

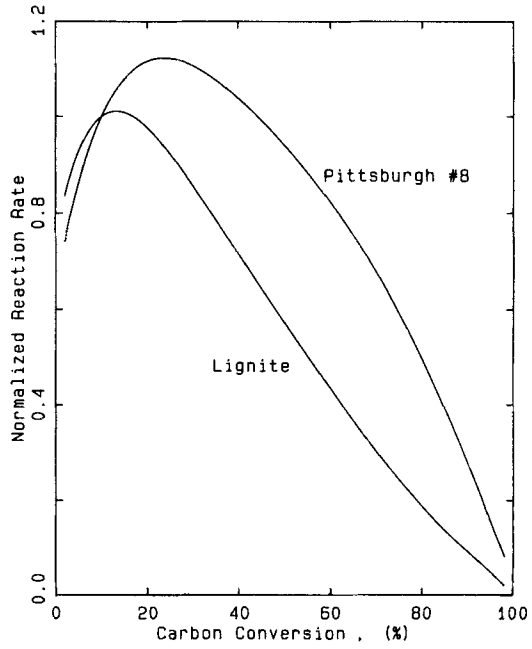

Figure 4. Experimentally obtained rate vs. conversion patterns for noncatalytic gasification of the two chars.

ditions (gaseous concentrations and temperatures) were employed during these investigations, resulting in reaction rates differing by well over an order of magnitude. Reaction conditions had no effect on the normalized rate vs. conversion patterns for all char-gas systems studied (*ibid.*), indicating that gasification took place under kinetic control. In addition, a lignite and a Pittsburgh #8 char exhibited almost identical rate vs. conversion patterns when each char was gasified with O_2, CO_2, or H_2O. That was not the case for another char produced from Illinois #6 coal, for which different reactivity patterns were observed during gasification with the three reactants. The changes in char reactivities were interpreted according to the pore structural evolution models developed earlier (Ballal and Zygourakis, 1987b).

Based on these results, the lignite and Pittsburgh #8 chars were selected for catalytic gasification studies. For comparison purposes, the rate vs. conversion patterns for the noncatalytic gasification of these two chars are depicted in Figure 4. The reaction rate increases initially for both chars, passes through a maximum, and decreases monotonically until complete conversion. Pittsburgh #8 char has considerably smaller micropore volume and surface area, and consequently the maximum in its reactivity is more pronounced and occurs at larger carbon conversion.

Char reactivities during catalytic gasification

The following sections present our experimental measurements regarding the catalytic effect of potassium carbonate on the reactivity of lignite and Pittsburgh #8 chars during gasification with air, CO_2, and water vapor. The fundamental kinetic mechanisms of catalytic gasification reactions are only briefly mentioned and no attempt is made to study them in detail. Rather, this work is aimed at investigating the magnitude of the catalytic effect at various loadings and its effect on the conversion-reaction rate relationship for different char-gas reactions using identical well-characterized char samples. Some aspects of previously proposed reaction mechanisms, however, were instrumental for the interpretation of experimental data.

Char-CO_2 Reaction. McKee and Chatterji (1975) studied the reaction of graphite with CO_2 in the presence of alkali metal carbonates. They suggested the following mechanism involving an overall oxidation-reduction cycle with the intermediate formation of alkali metal, *M*.

$$M_2CO_3 + 2\,C \rightarrow 2\,M + 3\,CO \qquad (1)$$

$$2\,M + CO_2 \rightarrow M_2O + CO \qquad (2)$$

$$M_2O + CO_2 \rightarrow M_2CO_3 \qquad (3)$$

Reactions 2 and 3 are likely to be relatively rapid and the overall rate is determined by reaction 1. Thermodynamic arguments were proposed for the presence of carbonate at higher temperature. Additional support for this mechanism comes from the release of alkali metal vapors that is reported to occur during these reactions. An alternate electrochemical mechanism was proposed by Jalan and Rao (1978), which assumes a continuous carbonate phase covering the carbon surface.

Figure 5 shows the effect of catalyst impregnation on the reaction rate-conversion relationship for the lignite char. CO_2 at 0.5 atm partial pressure was used and the reaction temperature

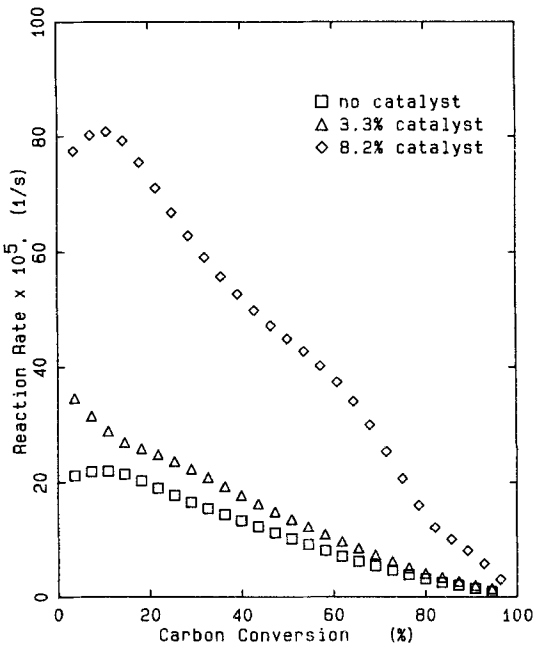

Figure 5. Experimental reactivity data for gasification of lignite char with CO_2 at various catalyst loadings.

was 822°C. The general evolution pattern of reaction rate with conversion did not change appreciably after catalyst impregnation. However, the magnitude of the reaction rate does increase indicating catalytic activity at all levels of conversion.

The effect of catalyst addition on the gasification of Pittsburgh #8 char (952°C, 0.5 atm partial pressure of CO_2) is presented in Figure 6. Very large enhancements in the reaction rate

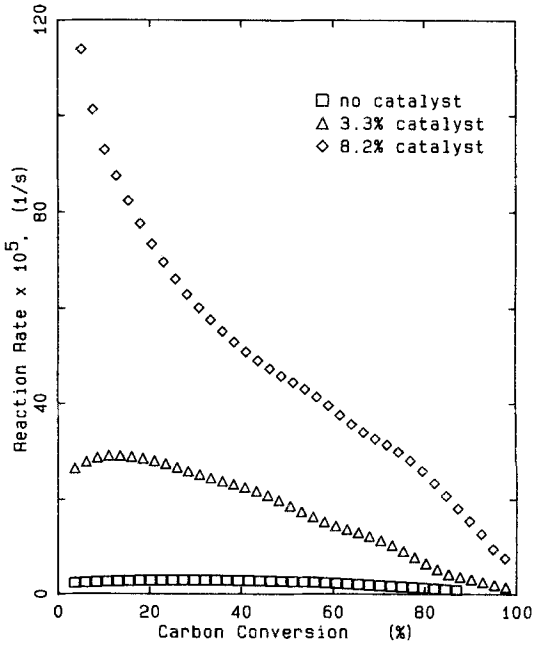

Figure 6. Experimental reactivity data for gasification of Pittsburgh #8 char with CO_2 at various catalyst loadings.

are seen, even when small amounts of catalyst were added. During noncatalytic gasification with CO_2, the reaction rate passes through a maximum at about 25% carbon conversion; this is not clearly seen in Figure 6 due to reduced scale. The pattern obtained for a 3.3 wt. % catalyst loading shows a slightly smaller maximum than the noncatalyzed char. With addition of 8.2 wt. % catalyst, the maximum in the reaction rate disappears completely and the rate exhibits a sharp decrease at low conversions.

Uneven catalyst dispersion may be the reason for the somewhat altered shape of the reactivity curve that was observed only at the highest catalyst loading and at low carbon conversions. Due to slower diffusion rates in this char, the catalyst is likely to be present at higher local concentrations at the particle exterior leading to the initial enhanced reaction rate. This effect, however, was observed only at the highest catalyst loading and it was considerably smaller than the drastic effect of nonuniform dispersion observed during the reacton of this char with oxygen. Despite the somewhat reduced catalytic activity at higher conversions, the rate enhancement due to catalyst addition was appreciable over the entire range of conversions.

Char-Water Reaction. Experimental investigations by McKee and Chatterji (1978) suggested a cyclic mechanism for the catalytic gasification of graphite with water vapor in the presence of alkali metal carbonates. According to their mechanism, the alkali metal is formed as an intermediate which readily reacts with water vapor to produce hydroxide that is finally converted back to carbonate in the presence of CO. The following reactions illustrate the overall mechanism.

$$M_2CO_3 + 2\,C \rightarrow 2\,M + 3\,CO \qquad (4)$$

$$2\,M + 2\,H_2O \rightarrow 2\,MOH + H_2 \qquad (5)$$

$$2\,MOH + CO \rightarrow M_2CO_3 + H_2 \qquad (6)$$

Reaction 4 is thought to be rate-determining. A similar mechanism was also suggested by Veraa and Bell (1978) for the gasification of coal-derived chars.

Figure 7 shows the effect of catalyst impregnation on the rate-conversion relationship for the lignite char. Gasification was carried out at 760°C in flowing N_2 containing 3% moisture. The magnitude of the reaction rate does increase with the addition of the catalyst at all conversions. Also, the rate-conversion pattern for the catalytic gasification is very similar to that obtained in the absence of catalyst. The maximum in the reaction rate curve becomes less pronounced with addition of catalyst, primarily due to nonuniformities in the distribution of catalyst. Again, the initial reaction rates are enhanced because of the large amounts of catalyst residing on the particle exterior.

The rate of catalytic gasification of the Pittsburgh #8 char at 884°C is depicted in Figure 8. Appreciable catalytic activity is seen at all levels of conversion. Once again, the rate-conversion pattern remains nearly unchanged even in the presence of catalyst. The catalytic enhancement of the gasification rate for this char is considerably larger than that obtained for the lignite char. This is in agreement with the analogous observation during the gasification of these two chars with CO_2.

Char-Oxygen Reaction. An oxygen transfer mechanism involving the oxidation-reduction cycle of alkali metal oxides was proposed by McKee and Chatterji (1975) for the catalytic combustion of graphite in the presence of carbonates of these metals. The carbonate decomposes into oxide that is further oxidized in the oxygen environment to produce higher oxides (mainly peroxide). Carbon then reduces the higher oxide to produce CO_2. The reactions may be written as follows.

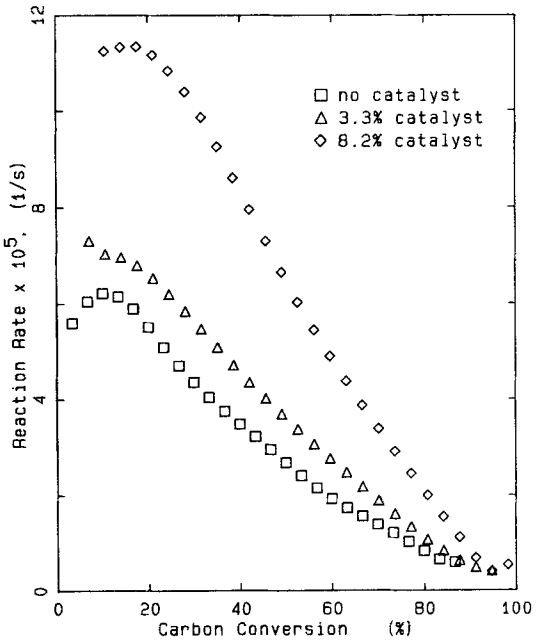

Figure 7. Experimental reactivity data for gasification of lignite char with H_2O at various catalyst loadings.

$$M_2CO_3 \rightarrow M_2O + CO_2 \qquad (7)$$

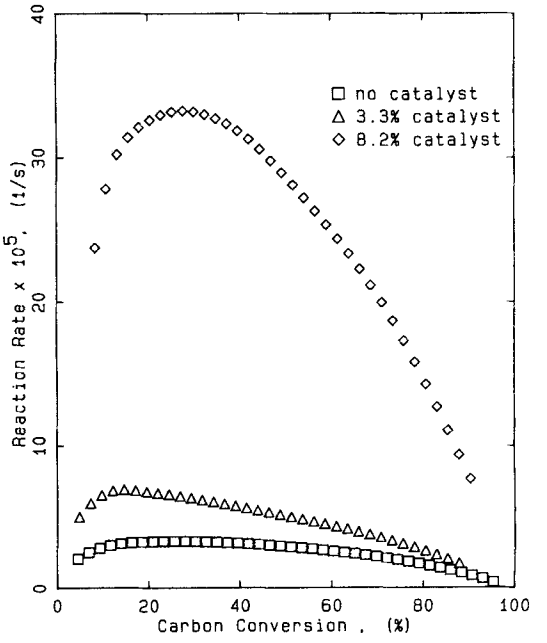

Figure 8. Experimental reactivity data for gasification of Pittsburgh #8 char with H_2O at various catalyst loadings.

$$2\,M_2O + O_2 \rightarrow 2\,M_2O_2 \qquad (8)$$

$$2\,M_2O_2 + C \rightarrow 2\,M_2O + CO_2 \qquad (9)$$

where M denotes the alkali metal. Thermodynamic arguments were put forward in favor of this mechanism. Alternate schemes have also been suggested in the literature and they appear to be appropriate at higher temperatures and in the presence of a continuous carbonate layer.

Figure 9 shows the effect of catalyst impregnation on the rate of combustion of lignite char in air at 405°C. A marked catalytic activity is seen at all levels of conversion. Also, the rate-conversion pattern does not change appreciably due to the addition of catalyst.

An interesting rate-conversion pattern was observed during the combustion of catalyst impregnated Pittsburgh #8 char, Figure 10. The combustion was carried out in air at 453°C. For a 3.3 wt. % loading of potassium carbonate, the reaction rate decreased drastically up to 25% carbon conversion, possibly after a small initial increase. At this stage, the rate was in fact smaller than the rate for noncatalytic combustion. At conversions larger than 25%, the reaction rate again increased slightly and passed through a maximum before decreasing monotonically up to complete conversion. Similar behavior was also seen for the char sample loaded with 8.2% potassium carbonate. The initial maximum in the reaction rate was larger and the rate decreased up to about 60% carbon conversion before another increase in the reaction rate.

This behavior can be explained on the basis of nonuniform catalyst distribution caused by the slower diffusional rates in the interior of the Pittsburgh char particles. The SEM studies revealed catalyst-rich regions near the particle exterior and in small neighborhoods around macropore cavities, while the rest of the particle contained negligible amounts of the catalyst.

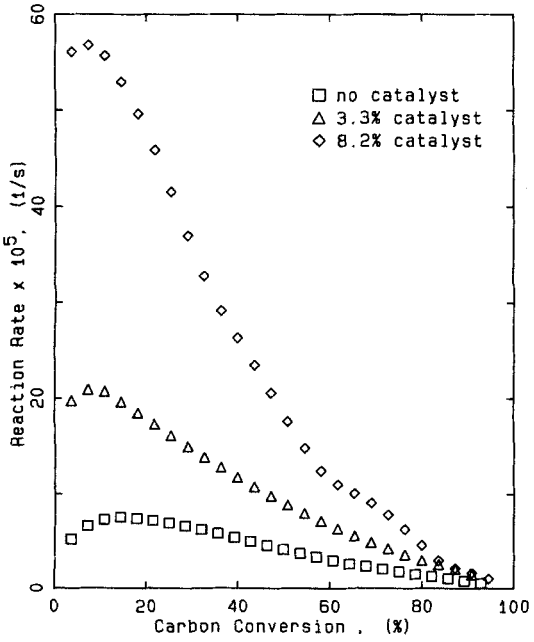

Figure 9. Experimental reactivity data for gasification of lignite char with O_2 at various catalyst loadings.

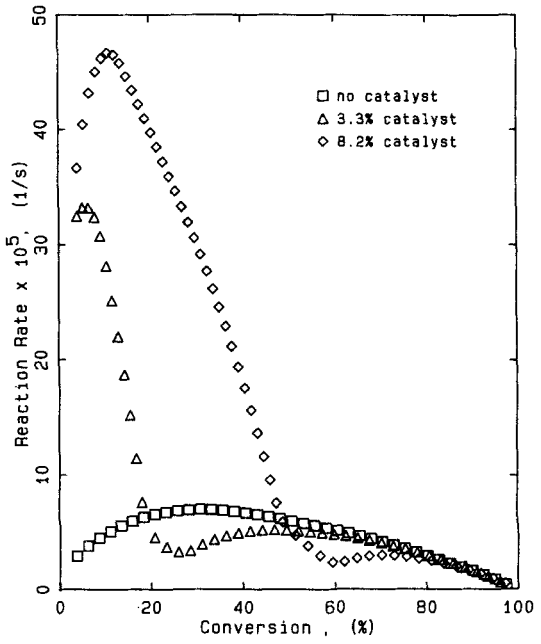

Figure 10. Experimental reactivity data for gasification of Pittsburgh #8 char with O_2 at various catalyst loadings.

Both the catalyst-rich and catalyst-lean regions contribute to the overall reaction rate. However, the overall rate observed during the initial stages of gasification is dominated by the contribution of catalyst-rich regions where the carbon is consumed rapidly due to its vastly enhanced reactivity. Thus, local carbon conversions in the catalyst-lean regions will still be very low when the carbon in the catalyst-rich regions is almost completely consumed. The overall rate after this point will be determined by the slower (essentially noncatalytic) reaction in the catalyst-lean regions.

This transition corresponds to the local minimum in the overall reaction rate observed in the reactivity curves for the catalyst-impregnated samples, Figure 10. After the local minimum, the observed rates increase again, pass through a maximum, and then decrease monotonically. Close examination of the catalyst-impregnated sample reactivity during this second stage of gasification revealed a pattern that is almost identical to the reactivity curve of the noncatalytic reaction.

Two additional observations must be made here. The experimental results indicate that local carbon conversions in the catalyst-lean region are very small at the local minimum of the reactivity curve—which occurs, for example, at about 25% overall carbon conversion for the 3.3 wt. % catalyst-impregnated char. Therefore, the overall observed rate at this conversion is almost equal to the initial rate for the noncatalytic gasification, as clearly seen in Figure 10. Note also that the noncatalytic gasification rate increases with conversion, passing through a maximum at about 30% conversion due to pore structure evolution effects. As a result, the noncatalytic rate at higher conversions is in fact larger than the observed reaction rate for the catalyst-impregnated samples at the local minimum where reaction in the catalyst-rich region is essentially completed. At higher catalyst loadings, the catalyst can permeate to greater depth inside the microparticles. The catalyst-rich region is correspondingly

larger, and hence the range of enhanced reaction rates extends up to higher carbon conversions.

It should be noted that a somewhat analogous phenomenon was observed during the gasification of the same char with CO_2, although only at the highest catalyst loading. However, it was considerably less pronounced than in the case of combustion. This may be explained on the basis of the higher reaction temperatures required for gasification with CO_2 and the different mechanisms followed by the char-O_2 and char-CO_2 reactions. The char-CO_2 reaction proceeds through the formation of potassium metal, which may be present in the form of vapor at the high reaction temperature. Hence, the catalyst is likely to redistribute itself more evenly throughout the particle even though the initial impregnation resulted in nonuniform catalyst dispersion. During combustion, however, the temperature is considerably lower and reaction proceeds through the intermediate formation of oxides (rather than metallic vapor). Thus, redistribution of the catalyst due to reaction is unlikely and the initial nonuniform distribution is maintained throughout the combustion process, leading to complex rate-conversion patterns. In the case of the lignite char studied here, even the initial dispersion of the catalyst is likely to be more uniform due to considerably faster diffusional rates in this char. Hence, the catalytic enhancement of the reaction rate is nearly uniform at all levels of conversion for gasification with both O_2 and CO_2 despite the possibly different reaction mechanisms.

Effect of Catalyst Loading on Char Reactivity. Figure 11 shows the effect of catalyst loading on the magnitude of the gasification rate for the lignite char. The catalytic enhancement (i.e., the ratio of the catalytic gasification rate over the corresponding rate in the absence of catalyst) is plotted against the atomic ratio of added potassium over the carbon present in the unreacted char. Since our earlier discussion, Figures 5–10, indicated that dissimilar catalytic enhancements may be observed at conversion levels for some chars, a comparison of initial reaction rates will indicate unrealistically large increases in char reactivities. In order to obtain more meaningful comparisons, the average reaction rates observed between 0 and 75% carbon conversion were used to compute the catalytic enhancements.

Moderate enhancement in the reaction rate is observed for the gasification of lignite char. Similar rate increases are observed for all three heterogeneous reactions. The catalyst is not expected to redistribute itself inside the particle during gasification with O_2, and the catalytic activity for this reaction indeed appears to level off slightly at higher loadings. A steady increase in the catalytic activity with loading is observed for the other two reactions, at least for the catalyst concentrations employed in this study.

Figure 12 depicts the magnitude of the catalytic activity of the Pittsburgh #8 char for all three char-gas reactions. Substantial catalytic enhancement is evident during its gasification with CO_2 and H_2O, while a relatively negligible increase in the average reactivity is observed during its reaction with oxygen. However, due to the drastic effect of uneven catalyst distribution in this char, Figure 10, the observed average catalytic enhancement factors for the combustion of these chars have only limited significance.

The Pittsburgh #8 char shows considerably higher catalytic activity as compared to the lignite char for char-CO_2 and char-H_2O reactions. Although a definitive answer for this observation cannot be given at present, it may be related to the large ash content (40%) of the lignite char. The rate of catalytic gasification with CO_2 and H_2O is controlled by the interfacial contact area between the catalyst particle and the carbon atoms on the surface (McKee, 1978). A major fraction of the surface area of the lignite char is already covered by the large amount of the inorganic impurities. This reduces the chances of interaction between the catalyst particle and the carbon atom on the surface. Consequently, lower enhancements in the gasification rate may be observed for the lignite char.

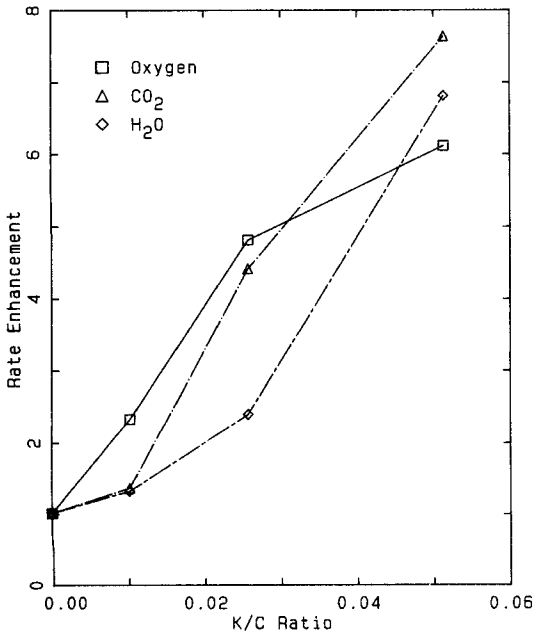

Figure 11. Effect of catalyst loading on gasification rate for lignite char.

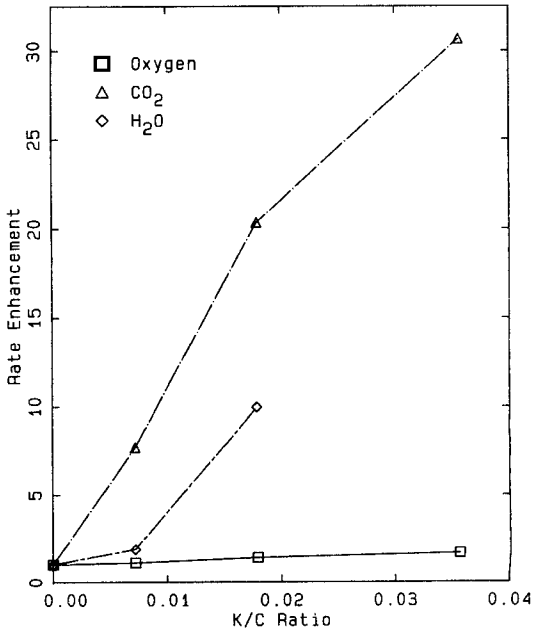

Figure 12. Effect of catalyst loading on gasification rate for Pittsburgh #8 char.

Conclusions

Well-characterized samples of two coal-derived chars, Pittsburgh #8 and Texas lignite, were impregnated with potassium carbonate from an aqueous solution. The effect of catalyst addition was evaluated for both chars by reacting identical char samples with carbon dioxide, water vapor, and oxygen. The Pittsburgh #8 char showed considerably larger catalytic enhancement, compared to the lignite char. For both chars, the maximum enhancement in reactivity was observed during gasification with CO_2, followed by the reactions with H_2O and O_2. The char-O_2 reaction, however, is considerably faster at typical gasification conditions than either the char-CO_2 or the char-H_2O reaction, even in the absence of a catalyst. Hence, the low catalytic activity observed during the char-O_2 reaction is not likely to be constraining for commercial applications.

The aqueous impregnation procedure resulted in intraparticle catalyst dispersions that depended strongly on the pore structure of char. Micropore capacities measured by CO_2 adsorption on both chars studied here did not change appreciably after cation addition, indicating insignificant blockage of fine micropores by the catalyst. On a macroscopic scale, however, significantly nonuniform dispersion resulted from the catalytic impregnation of the Pittsburgh #8 char. Since the macropore structure of this char consists of a few large cavities with few interconnections, large resistances to the transport of catalyst were encountered during impregnation and resulted in a highly nonuniform catalyst distribution.

The effects of nonuniform dispersion were most pronounced during the combustion of the Pittsburgh #8 char with oxygen. The catalyst did not exhibit any intraparticle mobility and its initially uneven distribution was maintained throughout the course of the reaction. Very high catalytic activity was observed at small conversions due to fast combustion of carbon in the catalyst-rich region. As the carbon in the catalyst-rich shell was exhausted, however, the catalytic activity disappeared entirely and gasification in the catalyst-lean regions appeared to be essentially noncatalytic.

When reacted with CO_2 or water vapor, however, the same char showed few signs of uneven distribution and exhibited large enhancements in reactivity. The catalyst appears to redistribute itself during gasification with CO_2 and H_2O, resulting in sustained superior catalytic effect at all conversions. Thus, the reaction mechanism and possibly the reaction temperature appear to be important factors affecting the catalyst dispersion and, consequently, the magnitude of the catalytic effect.

The possible redistribution of catalyst during gasification with CO_2 and H_2O has important practical ramifications. Uniform catalytic dispersion is usually desirable to achieve sustained enhancements in gasification rates. More elaborate impregnation techniques could be employed to obtain uniform initial intraparticle distribution of the catalyst. Economic considerations, however, may preclude the use of such techniques for chars with dense pore structures. In such cases, the possible redistribution of the catalyst during gasification will play an important role. The catalyst, although unevenly distributed initially, may redistribute itself during gasification, leading to large increases in the char reactivity over the entire range of conversions. Thus, superior and sustained catalyst performance could be realized using inexpensive impregnation techniques despite the nonuniformities in the initial catalytic distribution.

Finally, the reported observations indicate the complexity of the catalytic gasification and the strong interplay between the pore structural and chemical effects underlying these processes. It is clearly imperative to examine the catalytic rate enhancements over the entire range of carbon conversions. Unrealistically large estimates may be inferred if only the initial char reactivities are employed for such comparisons. Moreover, due to the different chemical mechanisms underlying the various char gasification reactions, the overall catalytic rate enhancement may be drastically different for these reactions even when they are carried out on the same char. It is therefore essential to study separately the various gasification reactions using chars with widely different chemical and physical structures in order to provide meaningful evaluations of catalyst performance.

Acknowledgment

This work was supported in part by a grant from the Robert A. Welch Foundation.

Literature Cited

Ballal, G. D., "A Study of Char Gasification Reactions," Ph.D. Diss., Rice Univ., Houston, TX (1985).

Ballal, G. D., and K. Zygourakis, "Kinetics of Char Gasification with Oxygen and Carbon Dioxide," *Chem. Eng. Commun.*, **49**, 181 (1986).

———, "Evolution of Pore Surface Area During Noncatalytic Gas-Solid Reactions. 2: Experimental Results and Model Validation," *Ind. Eng. Chem. Res.*, **26**, 1787 (1987a).

———, "Evolution of Pore Surface Area During Noncatalytic Gas-Solid Reactions. 1: Model Development," *Ind. Eng. Chem. Res.*, **26**, 911 (1987b).

Glass, M. W., and K. Zygourakis, "Macropore Size Analysis Using Digital Image Processing and a Stereological Model," submitted, *Chem. Eng. Commun.* (1987).

Huhn, F., J. Klein, and H. Juntgen, "Investigations on the Alkali-Catalyzed Steam Gasification of Coal. Kinetics and Interactions of Alkali Catalyst with Carbon," *Fuel*, **62**, 196 (1983).

Jalan, B. P., and Y. K. Rao, "A Study of the Rates of Catalytic Boudouard Reaction," *Carbon*, **16**, 175 (1978).

McKee, D. W., "The Catalyzed Gasification Reactions of Carbon," *Chemistry and Physics of Carbon*, 16, P. L. Walker, P. A. Thurber, eds., Marcel Dekker, New York (1981).

McKee, D. W., and D. Chatterji, "The Catalytic Behavior of Alkali Metal Carbonates and Oxides in Graphite Oxidation," *Carbon*, **13**, 381 (1975).

———, "The Catalyzed Gasification of Graphite with Water Vapor," Carbon, **16**, 53 (1978).

Spiro, C. L., D. W. McKee, P. G. Kosky, and E. J. Lamby, "Catalytic CO_2 Gasification of Graphite vs. Coal Char," *Fuel*, **62**, 180 (1983).

Su, J. L., and D. D. Perlmutter, "Porosity Effects on Catalytic Char Oxidation: A Catalyst Deposition Model," *AIChE J.*, **31**, 957 (1985a).

———, "Porosity Effects on Catalytic Char Oxidation: Experimental Results," *AIChE J.*, **31**, 965 (1985b).

Veraa, M. J., and A. T. Bell, "Effects of Alkali Metal Catalysts on Gasification of Coal Char," *Fuel*, **57**, 194 (1978).

Wen, W. Y., "Mechanisms of Alkali Metal Catalysis in the Gasification of Coal, Char or Graphite," *Catal. Rev. Sci. Eng.*, **22**, 1 (1980).

Manuscript received June 5, 1987, and revision received Oct. 15, 1987.